The role of transient surface morphology on composition control in AlGaN layers and wells

Cite as: Appl. Phys. Lett. **114**, 031602 (2019); https://doi.org/10.1063/1.5063933
Submitted: 02 October 2018 . Accepted: 20 December 2018 . Published Online: 23 January 2019

J. Houston Dycus, Shun Washiyama, Tim B. Eldred, Yan Guan, Ronny Kirste, Seiji Mita, Zlatko Sitar, Ramon Collazo, and James M. LeBeau

Applied Physics Letters ARTICLE scitation.org/journal/apl

The role of transient surface morphology on composition control in AlGaN layers and wells

Cite as: Appl. Phys. Lett. **114**, 031602 (2019); doi: 10.1063/1.5063933
Submitted: 02 October 2018 · Accepted: 20 December 2018 · Published Online: 23 January 2019

J. Houston Dycus,[1] Shun Washiyama,[1] Tim B. Eldred,[1] Yan Guan,[1] Ronny Kirste,[2] Seiji Mita,[2] Zlatko Sitar,[1,2] Ramon Collazo,[1] and James M. LeBeau[1,a)]

AFFILIATIONS

[1] Department of Materials Science and Engineering, North Carolina State University, Raleigh, North Carolina 27695-7907, USA
[2] Adroit Materials, Inc., 2054 Kildaire Farm Road, Suite 205, Cary, North Carolina 27518, USA

[a)] jmlebeau@ncsu.edu

ABSTRACT

The mechanisms governing "compositional pulling" during the growth of $Al_xGa_{1-x}N$ wells are investigated. Gallium-rich $Al_xGa_{1-x}N$ wells grown on high dislocation density AlN/sapphire templates exhibit asymmetric and diffuse composition profiles, while those grown on low dislocation density native AlN substrates do not. Furthermore, strain in all $Al_xGa_{1-x}N$ wells is found to be pseudomorphic, ruling it out as the dominating driving force. Rather, the high threading dislocation density of the AlN template is considered to play the defining role. We propose that a transient surface morphology is introduced during dislocation mediated spiral growth, which, in conjunction with process supersaturation, determines the Ga incorporation. These findings provide insights into compositional pulling in high Ga content $Al_xGa_{1-x}N$ grown on AlN and provide a route to grow thicker wells with very abrupt interfaces on native AlN substrates.

Group III-nitrides have become prevalent in optoelectronic applications, including LEDs and lasers, due to their wide bandgaps and efficiencies. As these devices move into the ultraviolet (UV) range and high power applications, $Al_xGa_{1-x}N$ wells are of particular interest.[1–5] To realize these applications, devices must have abrupt interfaces and precise compositional control, which can be challenging. Highly mismatched $Al_xGa_{1-x}N$ wells on AlN or GaN templates, for example, are found to grow with intermediate and/or gradient layers of composition that form spontaneously.[6] This phenomenon has been referred to as "compositional pulling" and can result in peak emission shifts, emission broadening, or double emission.[7] Furthermore, compositional pulling has been a major challenge when trying to grow high quality, pseudomorphically distributed Bragg reflectors (DBRs) for $Al_xGa_{1-x}N$-based devices.[8–10]

Compositional pulling is thought to result from the rejection of Ga atoms at the growth front due to strain.[6,11] The strain is then accommodated by forming layers that reduce the total strain energy via tension and compression within the subdivided layers.[6] Given that pulling occurs for $Al_xGa_{1-x}N$ wells grown on GaN or AlN templates, strain may not fully explain the observed behavior. For example, surface morphology can also play a key role in controlling Ga incorporation. On substrates with moderate to high dislocation density, the resulting $Al_xGa_{1-x}N$ thin film composition depends strongly on the substrate miscut and species supersaturation.[12] Depending on these variables, the film composition can vary by even 100%. Therefore, the influence of process and substrate selection on compositional uniformity in $Al_xGa_{1-x}N$ warrants further investigation.

In this letter, the role of substrate dislocation density in defining the composition profiles of AlN–$Al_xGa_{1-x}N$ superlattices is investigated. Using aberration corrected scanning transmission electron microscopy (STEM), compositional pulling is found to occur when $Al_xGa_{1-x}N$ wells are grown on relaxed AlN templates on sapphire, which contains a high density of dislocations, but does not arise on low defect AlN single crystals. Contrary to the strain derived mechanism, the $Al_xGa_{1-x}N$ wells are pseudomorphic on both substrates. For AlN templates, a transient surface morphology resulting from the high dislocation content and the Ga precursor is proposed to mediate compositional pulling. These findings provide insights into compositional pulling in high Ga content $Al_xGa_{1-x}N$ layers and show that it can be prevented by ensuring uniform substrate steps and step-flow growth.

AlN substrates with a surface dislocation density of 10^3/cm^2 were processed from AlN boules grown by physical vapor transport[13,14] with a pre-epitaxial, acid-based AlN surface preparation outlined in Ref. 15. AlN templates on sapphire were prepared as described in Ref. 16 with a 10^9/cm^2 dislocation density. The AlN template lattice parameter was identical to bulk AlN, which indicated that it was fully relaxed (see supplementary material, Fig. S1). The $Al_xGa_{1-x}N$ well superlattices were grown on both substrate types simultaneously in the same MOCVD chamber to limit the external variables of growth. Four groups of 4× $Al_xGa_{1-x}N$/AlN barrier superlattices were grown during the process with the increasing nominal Ga composition: SL 1 $Al_{0.9}Ga_{0.1}N$/AlN, SL 2 $Al_{0.7}Ga_{0.3}N$/AlN, SL 3 $Al_{0.5}Ga_{0.5}N$/AlN, and SL 4 $Al_{0.3}Ga_{0.7}N$/AlN. The intended well thicknesses were 17 nm for SL1 and 8 nm for SL2, SL3, and SL4. The AlN barriers were all 17 nm thick. Each SL group was then separated by an ∼200 nm thick AlN spacer, as shown schematically in Fig. 1(a). A 50 nm thick GaN cap was grown as a last step. The total gas pressure in the reactor was kept constant at 20 Torr throughout the growth process. Trimethylaluminum (TMA), triethylgallium (TEG), and ammonia were used as Al, Ga, and N precursors, respectively. All $Al_xGa_{1-x}N$ layers were grown at a substrate temperature of 1100 °C in H_2 diluent gas with a total reactor flow of 10 slm. V/III ratios during $Al_xGa_{1-x}N$ SLs were varied from 260 to 530 while maintaining a constant ammonia flow rate of 0.3 slm. To further explore the influence of dislocation density, an additional sample was grown on a higher dislocation content AlN template on sapphire (10^{10}/cm^2, as estimated from STEM).

Samples for electron microscopy were prepared by the Si-stacking method[17] with conventional wedge polishing.[18] Low energy ion milling with a Fischione 1050 TEM mill was used for final thinning. For STEM imaging and spectroscopy, a probe-corrected FEI Titan G2 60–300 kV S/TEM operated at 200 kV was used. The probe forming convergence semi-angle was 14 mrad, and the annular dark-field inner semi-angle was 77 mrad. Images were acquired with the revolving STEM (RevSTEM) method to minimize measurement error due to sample drift.[19–22] For each RevSTEM series, 20 frames were collected with a dwell time of 0.5 μs and a 90° rotation between each frame. Bruker Espirit was used for energy dispersive X-ray spectroscopy (EDS) with a FEI Super-X detector, and drift correction was applied between each frame. The Ga–K and Al–K characteristic X-rays were used for elemental quantification.

HAADF STEM image intensities increase with the increasing Ga content and thus provide a direct, qualitative assessment of composition across each superlattice. As shown in Fig. 1(b), the $Al_xGa_{1-x}N$ wells exhibit a vastly different Ga distribution and thicknesses depending on the substrate and the target composition. On the AlN template, SLs 1 and 2 have abrupt interfaces throughout, but the intensity profile becomes more complicated as the target Ga content increases (SLs 3 and 4). Starting at SL 3 [Fig. 1(b), left], distinct layers are observed within each $Al_xGa_{1-x}N$ well which vary in thickness. By increasing the Ga content further, SL4, the thickness of the intermediate layers increases to 10–20 nm. In stark contrast, the well/barrier interfaces on the AlN single crystal substrate are all abrupt.

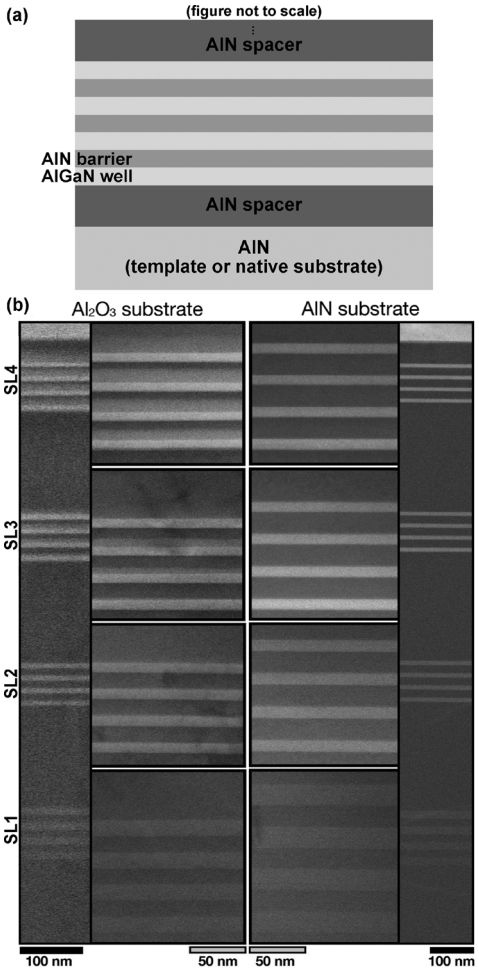

FIG. 1. (a) Schematic of the first superlattice grown on either an AlN template or native AlN. (b) HAADF-STEM of the AlGaN superlattices grown on an AlN template on sapphire (left) and an AlN native substrate (right). Brighter intensity indicates the higher Ga content. The images have been aligned to the start of each SL to emphasize the difference in the growth rate. Compositional pulling occurs only for SLs 3 and 4 for the AlN template on sapphire. Note that the size of the scale bars is different to account for the difference in growth rates.

As the thin films grown here contained multiple SLs, each with different Al/Ga contents, X-ray diffraction could not be used for reliable composition quantification (see supplementary material Fig. S2). Using EDS, the average peak compositions for SLs 1–4 are determined to be 91, 70, 45, and 27 at. % Al, respectively, and are found to be in very good agreement with the target compositions. Similarly, on the AlN single crystal, the average peak compositions for SLs 1–4 are found to be 92, 76, 55, and 42 at. % Al, which are higher than on sapphire. Furthermore, these results indicate that the composition of SL3 on the AlN template is most comparable to SL4 grown on the native AlN substrate.

The thin film growth rates also depend strongly on the substrate selection and the target Ga content. As shown in Table I, the layers grown on the native AlN substrate were all

TABLE I. Superlattice and spacer layer thicknesses for films grown on the AlN template and native AlN substrates. The thickness ratio is defined as native/template.

	Template (nm)	Native (nm)	Ratio
SL 1	82	125	1.52
Spacer 1	160	246	1.54
SL 2	66	100	1.52
Spacer 2	160	244	1.52
SL 3	80	96	1.2
Spacer 3	161	247	1.53
SL 4	74	88	1.19

considerably thicker than those on the AlN template. The observed difference in the AlN growth rates is an extrinsic effect due to non-uniformities in this particular growth run, namely, differences in the sample size and lack of sample rotation. This is evidenced by the initially constant thickness ratio–1.53 ± 0.01 (native/template)–for the spacers and SLs 1/2 on both substrates, i.e., when pulling does not occur. The growth rate, however, accelerates by ~20% for the template when pronounced pulling occurs (AlN templates SL 3 and SL 4). This behavior indicates that there is an altered growth mode within the high Ga content wells and suggests a key role in substrate selection for controlling the evolution of Ga incorporation.

To examine the differences in strain states between films on the two substrates, accurate and precise lattice parameters are directly measured in real-space using RevSTEM.[19] The out-of-plane lattice parameters of the $Al_{0.5}Ga_{0.5}N$ well, which exhibits significant pulling, are shown in Fig. 2. The major difference is that the well grown on the AlN template exhibits a diffuse, decreasing lattice parameter into the barrier, and corresponds to the intermediate layer seen in HAADF STEM intensity. In contrast, the out-of-plane parameter for the equivalent composition on the native AlN substrates returns immediately to that for the AlN barrier (498 pm). Furthermore, the projection-corrected, in-plane lattice parameter is 311 pm in both cases and is in excellent agreement with bulk AlN (311.2 pm). Films grown on both the template and the native substrate thus remain pseudomorphic, which is further supported by reciprocal space maps provided in supplementary material Fig. S3.

The strain energy U can be estimated by using $U = 1/(s_{11} + s_{12})((a - a_0)/a_0)^2$, where s_{11} and s_{12} are the elastic compliances in the c-plane and a and a_0 are the lattice parameters of the strained and relaxed layers, respectively.[23] For the highest Ga composition well, $Al_{0.3}Ga_{0.7}N$, which is biaxially strained to AlN, the strain energy is 0.13 kcal/mol. This is rather small compared to that of surface gas reactions that are on the order of 10 kcal/mol.[24–27] Therefore, the strain energy can be regarded as insufficient to dominate the observed growth behavior as both samples exhibit similar strain states, but very different Ga compositional profiles.

Beyond strain, threading dislocations may play an important role in defining compositional pulling. Their densities are dramatically different for the two substrates: ~10^9–10^{10}/cm^2 for AlN templates on sapphire and ~10^3/cm^2 for native AlN substrates. To gauge the influence of dislocation density on compositional

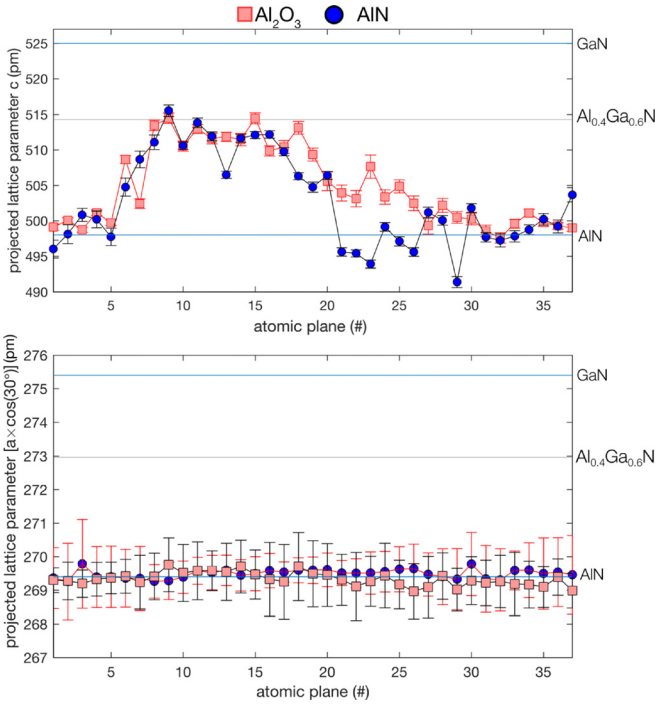

FIG. 2. Lattice parameter measurements across individual wells in QW3 and QW4 for the AlN template (squares) and native (circles) substrates.

pulling, a SL stack was grown on the AlN template with a higher surface dislocation density of ~10^{10}/cm^2, presented in Figs. 3(a) and 3(b). The extent of the transition layers is now exaggerated and enables a full accounting of the Ga compositional profile features. Notably, an intermediate step in the HAADF STEM intensity, and thus Ga composition, occurs at the AlN spacer → well transition. While this initial transition also occurs at the barrier → well interfaces, it is the thickest at the first well. In contrast, the well → barrier transition thickness increases for each well in the sequence. After growth of the final SL well, the transition region exhibits a much broader decay of Ga into the spacer. In contrast, the wells grown on native AlN show abrupt transitions across the entire SL, as shown in Figs. 3(a) and 3(c).

From Figs. 1–3 and Table I, the pulling behavior is summarized as follows: (1) regardless of the substrate selection, the wells are pseudomorphic to AlN, (2) compositional pulling in $Al_xGa_{1-x}N$ wells on AlN templates increases with the Ga target concentration, (3) compositional pulling is not observed in any of the $Al_xGa_{1-x}N$ wells grown on native AlN substrates, (4) the spacer → well transition layer is thicker than that of the barriers → wells (AlN template only), and (5) a broad Ga concentration decay occurs at well → spacer transition (AlN template only). Importantly, these features cannot be adequately described by the surface segregation Muraki model[28] that is governed by a strain energy barrier needed for Ga incorporation. In that model, the composition profile follows a simple power law behavior, and it cannot describe the knee-like compositional pulling in the $Al_xGa_{1-x}N$ layers reported here. Rather, the behavior can be modeled using a double sigmoid function

$$x_n = \begin{cases} x_n = x_0\left[\exp\left\{-\left(\frac{n}{c_0}\right)^{-W_0}\right\}\right] + x_1\left[1-\exp\left\{-\left(\frac{n}{c_1}\right)^{W_1}\right\}\right] & (0 < n < N_1; \text{well}) \\ x_n = x_2\left[1-\exp\left\{-\left(\frac{n-N}{c_2-N}\right)^{-W_2}\right\}\right] + x_3\left[\exp\left\{-\left(\frac{n-N}{c_3-N}\right)^{W_3}\right\}\right] & (n > N; \text{barrier}), \end{cases} \quad (1)$$

where x_i is the maximum composition in each stage, W_i is the "transition rate" in each stage, and c_i is the center of each transition. The model provides a near perfect fit across an entire SL exhibiting compositional pulling, as shown in Fig. 3(b). Fit parameters are provided in supplementary material, Table S1. The key feature is that the compositional profile requires a two-step process, i.e., a transient, to explain the observed Ga distribution.

Based on the observed behavior of compositional pulling and the lack of a difference in the strain state, alternative mechanisms beyond should be considered. In particular, dislocations can mediate growth through a wide variety of surface morphologies as a function of supersaturation.[12,15] The high dislocation content of the AlN templates, for example, leads to spiral growth mediated by screw dislocations.[29] On the native AlN, the $Al_xGa_{1-x}N$ film surface exhibits step flow growth. According to BCF theory of spiral growth,[29] supersaturation, σ, is inversely proportional to $1/\ln(1+\sigma)$, where λ_0 is the growth spiral terrace width. Upon introducing the Ga precursor, and thus Ga supersaturation, the spiral velocity increases. The concomitant decrease in the terrace width then changes the Ga incorporation, x_{Ga}, proportional to $A/(A + B\lambda_0)$, where A/B are constants determined by the precursor flow.[12] This relationship indicates that a decrease in the terrace width leads to a subsequent increase in Ga incorporation,[30] where a transient change in surface morphology results in a transient degree of Ga incorporation. The dislocation content paired with Ga supersaturation can thus play a dominant role in controlling Ga composition.

To support this hypothesis, Fig. 4 shows the evolution of the film surface immediately before and after growth of a single $Al_{0.6}Ga_{0.4}N$ well on an AlN template. The surface morphology changes significantly during the 10 nm layer growth. By visual inspection, the terrace width is found to be significantly decreased, leading to an increase in the Ga incorporation rate during this growth. For the well structures, this change in surface morphology would therefore lead to the two-stage transient spacer/barrier → well transitions (Fig. 3). For the well → barrier transition, the surface morphology again changes as it becomes simply determined by the Al supersaturation and accumulated Ga at the growth front (Ga precursor gas turned off). This then leads to the observed knee-shaped well → barrier transition. The evolving surface morphology also explains the asymmetric composition profile across the stack. By the start of each well within the SL, the surface does not return entirely to that at the start of the SL growth. If, however, sufficient AlN growth occurs before the start of the next well, such as at the well → spacer, a smoother decay in Ga incorporation is seen as the surface returns to the Al supersaturation determined morphology.

These findings indicate that the AlGaN surface morphology is predominately influenced by the low, commonly used, Ga supersaturation, in contrast to observations that changing Al supersaturation under typical growth conditions does not.[30,31] For screw dislocation mediated spiral growth on the AlN template, step density can be adjusted via Ga supersaturation where higher step density incorporates more Ga. For the low dislocation density native AlN, miscut controls the step density, and bilayer growth morphology is maintained throughout the growth

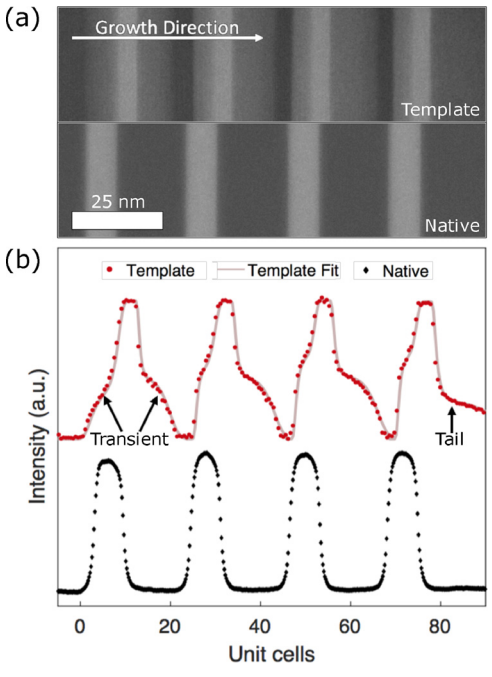

FIG. 3. (a) HAADF-STEM images of a superlattice grown on an AlN template with a high density of dislocations and on the native AlN substrate as indicated. (b) Integrated line profiles from (a) and the accompanying fit of the two-stage growth model described by Eq. (1) to the AlN template data.

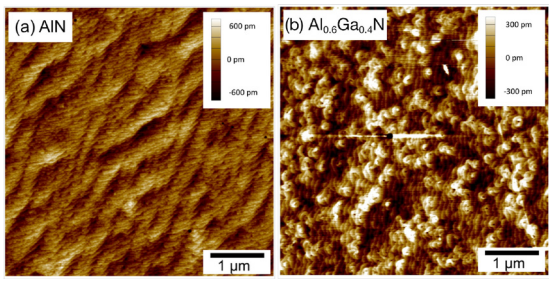

FIG. 4. Atomic force microscopy images of an (a) AlN template surface before growth of superlattices. (b) Surface of the same sample after a 10 nm growth of $Al_{0.6}Ga_{0.4}N$.

process regardless of Ga supersaturation.[15] Thus, strong compositional pulling does not occur when growing on native AlN substrates, even though the strain state of the wells is the same.

While high performance devices have been grown on AlN templates, those prior studies focused on quantum wells that are only a few nanometers thick where the growth surface would remain within the first transient and cannot be clearly observed.[2,5,32,33] Composition gradients have, however, also been identified within $Al_xGa_{1-x}N$ quantum wells and thicker films, leading to alternative MOCVD growth approaches such as pulsed atomic-layer epitaxy and migration enhanced MOCVD to prevent such gradients.[34,35] The wells grown here are on the order of 10–30 nm including pulling, which depends on the target Ga composition. Furthermore, pulling only occurs when Ga content is high. Thus, these results present an extreme in compositional pulling for such superlattices. Although not necessarily applicable to quantum wells in the active regions of UV lasers or light emitting diodes, superlattices like these are used for epitaxial distributed Bragg reflectors as typically used in vertical optically confined cavities.[36]

Based on the evidence, we conclude that compositional pulling cannot be explained by strain alone, but rather by a transient growth surface morphology governed by Al/Ga supersaturations and threading dislocation density. This occurs due to the spiral dominated growth on the AlN templates on sapphire that leads to a changing amount of Ga incorporation. In contrast, for the AlN substrate, the surface morphology does not change during growth due to its low dislocation density and bilayer growth mode. As a next step, these results point to the dynamic control of growth supersaturation to prevent compositional pulling on high dislocation density substrates. Given the large differences in compositional profiles, photoluminescence studies on single composition $Al_xGa_{1-x}N$ well superlattices grown on native AlN substrates can provide further insights into the impact of compositional pulling on optical properties.

See supplementary material for X-ray diffraction data for the AlN template sample and composition profile fit parameters.

We would like to thank Dr. Rafael Dalmau from HexaTech Inc. for helping in XRD analysis. We gratefully acknowledge support from NSF (ECCS-1508854, ECCS-1610992, DMR-1508191, and ECCS-1653383), ARO (W911NF-15-2-0068 and W911NF-16-C-0101), AFOSR (FA9550-17-1-0225 and FA9550-14-1-0182), DOE (DE-SC0011883), and ONRG NICOP (N62909-17-1-2004). J.H.D. acknowledges support for this work by the National Science Foundation Graduate Research Fellowship (Grant No. DGE-1252376). This work was performed in part at the Analytical Instrumentation Facility (AIF) at North Carolina State University, which is supported by the State of North Carolina and the National Science Foundation (Award No. ECCS-1542015). The AIF is a member of the North Carolina Research Triangle Nanotechnology Network (RTNN), a site in the National Nanotechnology Coordinated Infrastructure (NNCI).

REFERENCES

[1]J. Xie, S. Mita, Z. Bryan, W. Guo, L. Hussey, B. Moody, R. Schlesser, R. Kirste, M. Gerhold, R. Collazo, and Z. Sitar, Appl. Phys. Lett. **102**, 171102 (2013).
[2]H. Hirayama, N. Maeda, S. Fujikawa, S. Toyoda, and N. Kamata, Jpn. J. Appl. Phys., Part 1 **53**, 100209 (2014).
[3]R. Collazo, S. Mita, J. Xie, A. Rice, J. Tweedie, R. Dalmau, and Z. Sitar, Phys. Status Solidi c **8**, 2031 (2011).
[4]J. Han, M. H. Crawford, R. J. Shul, J. J. Figiel, M. Banas, L. Zhang, Y. K. Song, H. Zhou, and A. V. Nurmikko, Appl. Phys. Lett. **73**, 1688 (1998).
[5]M. Shatalov, W. Sun, A. Lunev, X. Hu, A. Dobrinsky, Y. Bilenko, J. Yang, M. Shur, R. Gaska, C. Moe, G. Garrett, and M. Wraback, Appl. Phys. Express **5**, 082101 (2012).
[6]B. Liu, R. Zhang, J. G. Zheng, X. L. Ji, D. Y. Fu, Z. L. Xie, D. J. Chen, P. Chen, R. L. Jiang, and Y. D. Zheng, Appl. Phys. Lett. **98**, 261916 (2011).
[7]M. Del P. Rodríguez-Torres, A. Y. Gorbatchev, V. A. Mishurnyi, F. De Anda, V. H. Mendez-García, R. Asomoza, Y. Kudriavtsev, and I. C. Hernandez, J. Cryst. Growth **277**, 138 (2005).
[8]C. He, Z. Qin, F. Xu, L. Zhang, J. Wang, M. Hou, S. Zhang, X. Wang, W. Ge, and B. Shen, Sci. Rep. **6**, 25124 (2016).
[9]H. Y. Lin, Y. F. Chen, T. Y. Lin, C. F. Shih, K. S. Liu, and N. C. Chen, J. Cryst. Growth **290**, 225 (2006).
[10]Y.-S. Liu, S. Wang, H. Xie, T.-T. Kao, K. Mehta, X. J. Jia, S.-C. Shen, P. D. Yoder, F. A. Ponce, and T. Detchprohm, Appl. Phys. Lett. **109**, 081103 (2016).
[11]N. Grandjean, J. Massies, and M. Leroux, Phys. Rev. B **53**, 998 (1996).
[12]I. Bryan, Z. Bryan, S. Mita, A. Rice, L. Hussey, C. Shelton, J. Tweedie, J.-P. Maria, R. Collazo, and Z. Sitar, J. Cryst. Growth **451**, 65 (2016).
[13]D. Zhuang, Z. Herro, R. Schlesser, and Z. Sitar, J. Cryst. Growth **287**, 372 (2006).
[14]P. Lu, R. Collazo, R. Dalmau, G. Durkaya, N. Dietz, B. Raghothamachar, M. Dudley, and Z. Sitar, J. Cryst. Growth **312**, 58 (2009).
[15]I. Bryan, Z. Bryan, S. Mita, A. Rice, J. Tweedie, R. Collazo, and Z. Sitar, J. Cryst. Growth **438**, 81 (2016).
[16]I. Bryan, Z. Bryan, S. Washiyama, P. Reddy, B. Gaddy, B. Sarkar, M. H. Breckenridge, Q. Guo, M. Bobea, J. Tweedie, S. Mita, D. Irving, R. Collazo, and Z. Sitar, Appl. Phys. Lett. **112**, 062102 (2018).
[17]J. Dycus and J. M. LeBeau, J. Microsc. **268**, 225 (2017).
[18]P. Voyles, J. Grazul, and D. Muller, Ultramicroscopy **96**, 251 (2003).
[19]J. H. Dycus, J. S. Harris, X. Sang, C. M. Fancher, S. D. Findlay, A. A. Oni, T.-T. E. Chan, C. C. Koch, J. L. Jones, L. J. Allen, D. L. Irving, and J. M. LeBeau, Microsc. Microanal. **21**, 946 (2015).
[20]A. A. Oni, X. Sang, S. V. Raju, S. Dumpala, S. Broderick, A. Kumar, S. Sinnott, S. Saxena, K. Rajan, and J. M. LeBeau, Appl. Phys. Lett. **106**, 011601 (2015).
[21]X. Sang and J. M. LeBeau, Ultramicroscopy **138**, 28 (2014).
[22]X. Sang, A. A. Oni, and J. M. LeBeau, Microsc. Microanal. **20**, 1764 (2014).
[23]B. Shen, T. Someya, and Y. Arakawa, Appl. Phys. Lett. **76**, 2746 (2000).
[24]A. Rice, R. Collazo, J. Tweedie, R. Dalmau, S. Mita, J. Xie, and Z. Sitar, J. Appl. Phys. **108**, 043510 (2010).
[25]J. R. Creighton, G. T. Wang, and M. E. Coltrin, J. Cryst. Growth **298**, 2 (2007).
[26]Q. An, A. Jaramillo-Botero, W. G. Liu, and W. A. Goddard, J. Phys. Chem. C **119**, 4095 (2015).
[27]I. Grzegory, J. Jun, M. Boćkowski, S. Krukowski, M. Wróblewski, B. Łucznik, and S. Porowski, J. Phys. Chem. Solids **56**, 639 (1995).
[28]K. Muraki, S. Fukatsu, Y. Shiraki, and R. Ito, Appl. Phys. Lett. **61**, 557 (1992).
[29]W.-K. Burton, N. Cabrera, and F. Frank, Philos. Trans. R. Soc. London A: Math., Phys. Eng. Sci. **243**, 299 (1951).
[30]S. Washiyama, "Al-rich AlGaN/AlN-based double barrier resonant tunneling diodes," Ph.D. thesis, North Carolina State University, 2018.
[31]S. Washiyama, P. Reddy, F. Kaess, R. Kirste, S. Mita, R. Collazo, and Z. Sitar, J. Appl. Phys. **124**, 115304 (2018).
[32]R. G. Banal, M. Funato, and Y. Kawakami, Appl. Phys. Lett. **99**, 011902 (2011).
[33]A. Bhattacharyya, T. D. Moustakas, L. Zhou, D. J. Smith, and W. Hug, Appl. Phys. Lett. **94**, 181907 (2009).
[34]J. P. Zhang, H. M. Wang, W. H. Sun, V. Adivarahan, S. Wu, A. Chitnis, C. Q. Chen, M. Shatalov, E. Kuokstis, J. W. Yang, and M. A. Khan, J. Electron. Mater. **32**, 364 (2003).
[35]R. S. Fareed, J. P. Zhang, R. Gaska, G. Tamulaitis, J. Mickevicius, R. Aleksiejunas, M. S. Shur, and M. A. Khan, Phys. Status Solidi C **2**, 2095 (2005).
[36]A. Franke, M. P. Hoffmann, R. Kirste, M. Bobea, J. Tweedie, F. Kaess, M. Gerhold, R. Collazo, and Z. Sitar, J. Appl. Phys. **120**, 135703 (2016).